CHARACTERIZATION OF LUNAR IMPACT CRATERS USING CHANDRAYAAN-2 HIGH-RESOLUTION POLARIMETRIC DUAL-FREQUENCY SAR DATA Deepak Putrevu*, Anup Das, Dharmendra Pandey, Tathagata Chakraborty, MS Tarun, VM Ramanujam, Shubham Gupta, Parikshit Parasher, Raghav Mehra, Gaurav Seth, Amit Shukla, Sanjay Trivedi, Rajeev Jyoti, Raj Kumar and the DFSAR Team
Space Applications Centre, Indian Space Research Organization, Ahmedabad, India *(dputrevu@sac.isro.gov.in)

Introduction: Earth based radars, such as Arecibo radio telescope observatory at Puerto Rico (S and P band) [1,2] and lunar orbiter based radars, such as Mini-SAR (S-band) on Chandrayaan-1 [3] and Mini-RF (S and X band) on Lunar Reconnaissance Orbiter (LRO) [4] due to their ability to probe few to several meters below the surface of the Moon have revealed many intriguing facts about the lunar surface. Dual Frequency Synthetic Aperture Radar (DFSAR) on Chandrayaan-2 (CH2) orbiter, the first lunar SAR system operating at L-band in addition to S-band, has shown potential to further the previous investigations and contribute significantly towards our understanding on the origin and evolution of lunar impact craters and associated physical processes.

The Instrument: DFSAR is capable of imaging lunar surface in stand-alone as well as joint modes at L-band (1.25 GHz) and S-band (2.5 GHz) [5] frequencies. The instrument can acquire images in single, dual, hybrid-circular and full polarimetric modes with resolution capacities from 2m to 75m in the slant range. The SAR system can be operated at incidence angles ranging from 9.6° to 36.9°. Major goal of the mission is to utilize full and hybrid polarimetric data for enabling unambiguous detection of water ice in the lunar poles. Further, the mission will help in characterizing lunar surface and shallow-subsurface geological features in dual microwave frequency bands.

Study Area and Data Used: For the present study L-band high resolution (azimuth 2.7m x slant range 2m) DFSAR data acquired in hybrid-circular polarimetric mode over a region (70.7°S, 22.5°E) near Simpelus crater in lunar south polar region (Fig. 1a) has been used. The region has prominent features showing three craters of different levels of weathering viz. fresh crater, partially degraded crater and highly degraded crater. For comparison, S-band SAR data from LRO Mini-RF and optical data from LRO Narrow Angle Camera (NAC) over the same region are used in the present study. Further, L-band full-polarimetric SAR observations over a secondary crater situated on the floor of Peary Crater (87.7°N, 31.1°E) in lunar north polar region (Fig. 3) has also been analysed to demonstrate the potential of full-pol over hybrid-pol data for crater ejecta distribution mapping.

Results: The present study exhibits some initial results obtained from data acquired by Chandrayaan-2 DFSAR instrument. Fig 1a and 1b show the Raney decomposed images [4] of L band DFSAR and S-band Mini-RF instruments, respectively.

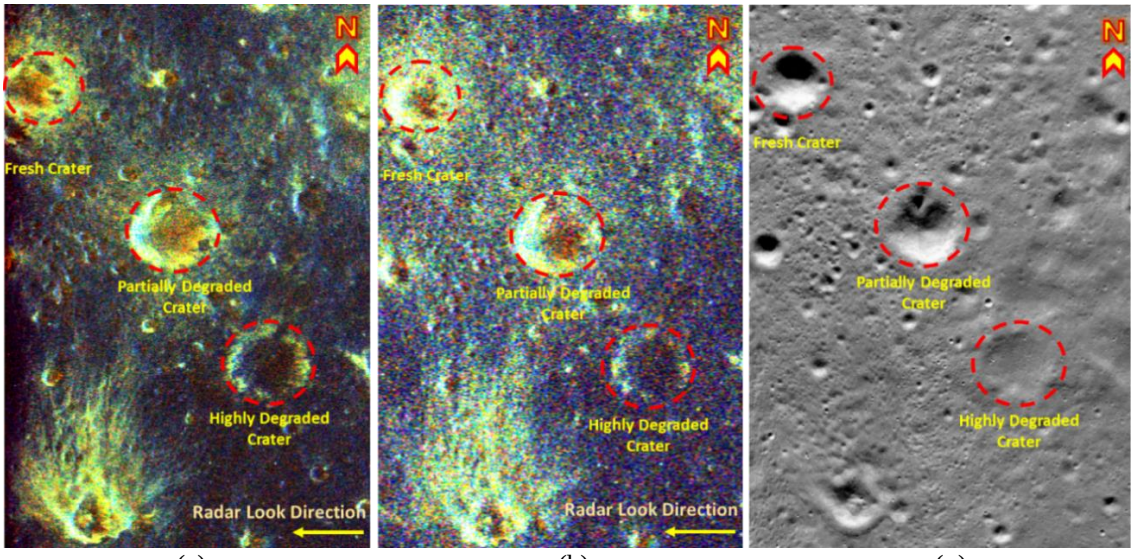

(a) (b) (c)

Figure 1 Raney (m-χ) decomposed image of study area acquired by (a) CH2 DFSAR L band; (b) LRO Mini-RF S band; (c) corresponding optical image acquired by LRO Narrow Angle Camera image

The DFSAR image due to high resolution (2m in slant range) shows numerous small craters not so apparent in Mini-RF data. The highly degraded crater in the region is identifiable in DFSAR data, whereas, in high resolution (0.5m pixel size) optical image (Fig 1c) from LRO NAC of the same region the crater is barely detectable.

Moreover, the ejecta distributions, as seen in bright yellowish tone around the craters in SAR images are not detectable in the optical image.

The mean Circular Polarization Ratios (CPR), indicative of radar wavelength scale roughness, were determined in Mini-RF (S-band) and DFSAR (L-band) data over interior and exterior part of the craters and presented in Fig. 2. The plot reveals that, CPR values in the exterior and interior part of the fresh crater are similar and highest among all the three craters. In the partially degraded crater, the interior part has higher CPR values than the exterior part of the crater and for the highly degraded crater, the exterior and interior CPR values are similar and lower compared to other types of craters.

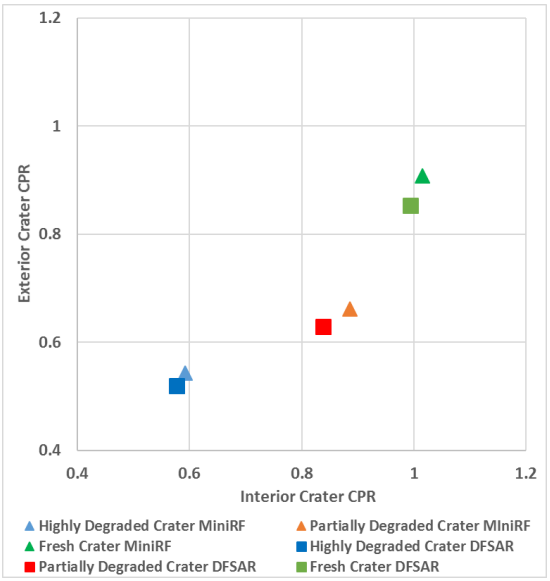

Figure 2 Average CPR values in the interior and exterior of the craters imaged by Mini-RF (S-band) and CH2 DFSAR (L-band). The *triangle* and *square* data points correspond to Mini-RF and DFSAR data, respectively.

The average CPR corresponding to the craters reveal many facts about the stages of evolution of these craters. While the crater is fresh, it is not exposed enough to space weathering. Due to this reason, the ejecta material is blocky and larger in size in both the interior and exterior part of the crater. However, with time the exterior of the crater experiences higher weathering in comparison to its interior. Hence, the ejecta present outside the crater are more fragmented and reduced in size. So, for partially degraded stage, the CPR of interior part is higher than the exterior part. For highly degraded crater, both interior and exterior parts are exposed to substantial space weathering leading to fineness of ejecta present in both the parts. Hence, the CPR in degraded crater is the lowest and alike in both interior and exterior parts.

In addition, the CPR values for the same crater is higher in S band (Mini-RF) compared to L band (DFSAR). The rock boulders which appear as prominent scatterers in S-band are not so in the L-band, owing to its wavelength. Hence, CPR is high in S band compared to L band.

Moreover, for fresh crater the difference of L and S band average CPR values is more in its exterior (0.05) compared to its interior (0.02). This indicates that, the internal part of the fresh crater is dominated by bigger rock blocks, equally sensitive to both L and S bands. On the contrary, for partially degraded crater, the mean CPR difference in L and S bands is higher in its interior (0.05) relative to its exterior (0.03). This relation may be due to reduction in the blocky nature of the interior part leading to variable sensitivity to different frequencies. Also, the exterior part is dominated by fine fragmented particles giving rise to almost similar CPR in both frequencies. Finally, for highly degraded crater, both its interior and exterior are dominated by fine fragmented particles resulting in identical CPRs in both L and S frequencies.

Further, radar backscatter of CH2 Full-Pol L-band SAR data over Lunar north polar region was determined (Fig. 3). The values show that, in co-pol data (HH and VV) the crater rim is prominent, but its ejecta is not clearly discernible. While, in the cross-pol channel (HV) both the crater rim and ejecta distributions are distinctly visible. Therefore, for delineation of the spatial distribution of ejecta in the interior and exterior of an impact crater, cross-pol data (HV or VH) is more valuable over linear co-pol data.

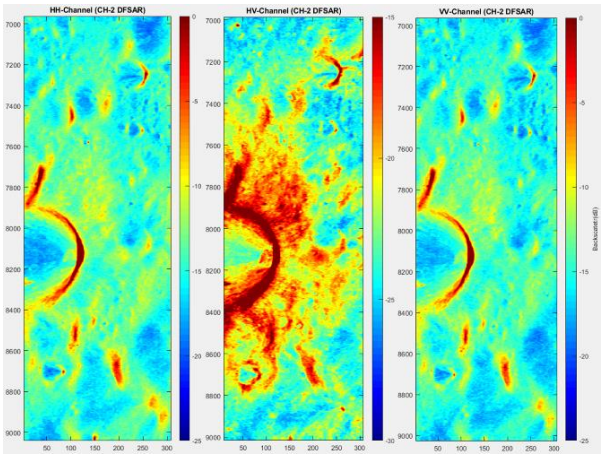

Figure 3 Radar backscatter for different polarization channels obtained from CH2 L-band Full-Pol SAR data. *Left:* HH, *Middle:* HV and *Right:* VV

References: [1] Cohen, M.H. (2009) *Journal of Astronomical History and Heritage, 12 (2),* pp. 141-152. [2] Thompson, T.W. et al. (2013) *The Radio Science Bulletin, 357,* pp. 23-35. [3] Spudis, P. D. et al. (2010) *Geophys. Res. Lett., 37,* L06204, doi:10.1029/2009GL042259. [4] Nozette, S. et al. (2010) *Space Science Reviews, 150*(1-4), 285-302. [5] Putrevu, D. et al. (2015) *Adv. Space Res.*, http://dx.doi.org/10.1016/j.asr.2015.10.029. [6] Raney, R. K. et al. (2012) *J. Geophys. Res., 117,* E00H21, doi:10.1029/2011JE003986.